



Design and Implementation of a Diagnostic Solid Propellant Fuel System Based on Laser Illuminator

Eng. Abdalrhman Adel¹, Prof. Osama A. Omer¹, Prof. M. Anwar², Prof. Mohammed Alamir³, Dr. Amir Almslmany^{4,*}

Citation:

Adel, A.; Osama, A.; Anwar, M.; Alamir, M.; Almslmany, A.

Inter. Jour. of Telecommunications, IJT'2023, Vol. 03, Issue 02, pp. 01-7, 2023.

Editor-in-Chief: Youssef Fayed.

Received: 25/08/2023.

Accepted: date 27/10/2023.

Published: date 05/11/2023.

Publisher's Note: The International Journal of Telecommunications, IJT, stays neutral regarding jurisdictional claims in published maps and institutional affiliations.



Copyright: © 2023 by the authors. Submitted for possible open access publication under the terms and conditions of the International Journal of Telecommunications, Air Defense College, ADC, (<https://ijt.journals.ekb.eg/>).

¹ Dept. of Elec. & Comm., faculty of engineering, Aswan University; abdou40105@gmail.com

¹ Dept. of Elec. & Comm., Faculty of engineering, Aswan University; omer.osama@aswu.edu.eg

² Faculty of Science, Aswan University Aswan, Egypt, melfawy99@aswu.edu.eg

³ Alexandria Higher Institute Engineering & Technology AIET; dr.mohammed.alamir@aiet.edu.eg

⁴ Dept. of Electronics & Comm., Egyptian Air Defense College; dr.mslmany.7256.adc@alexu.edu.eg

*Correspondence: dr.mslmany.7256.adc@alexu.edu.eg; Tel.: (+20-01120000739)

Abstract: In this paper, solid rocket fuel titration by non-destructive ultrasonic test, using ultrasonic laser receptor technology. This technique is one of the modern ways to receive ultrasound, this technology works by making a three-dimensional image of heterogeneous cracks. Taking into account mainly the storage temperature ranging from 50 to 70 C and the casings in which the rocket fuel is placed. Experiments were carried out on plastic and stainless steel covers. The thickness of plastic casings ranges from 16 to 17.5 mm. The thickness stainless steel ranges from 9 to 20.40 mm. The important scientific contribution of this research is testing the storage of rocket fuel at high temperatures and knowing what happens by introducing rocket fuel in the case of storage at those temperatures. To take into account the good ventilation system for solid rocket fuel.

Keywords: NDT; SPF; PRM.

1. Introduction

There are many distinct solid propellant combinations; however there are two primary categories that can be identified: homogeneous solid propellants and heterogeneous solid propellants. The fuel and oxidizer are often found in the same molecule in a homogenous combination [4]. No molecules larger than macro-level exist in the combination. Single-base and double-base homogeneous solid propellants can be distinguished from one another. There is just one kind of propellant base—typically nitrocellulose—in single-base propellants. Nitrocellulose and nitroglycerin are typically the two types of molecules that make up the propellant base in double-base propellants. Heterogeneous, or composite, propellants are made up of many materials for the fuel and oxidizer [5]. The most often utilized combination is powdered aluminum as the fuel and ammonium perchlorate (AP) as the oxidizer. Ideal solid propellants would cure with no further chemical or physical changes after being blended and shaped into their final shape. The propellant will really continue to undergo chemical changes, which will cause the mechanical characteristics to change as well. The breakdown of the binder, which is often hydroxyl-terminated polybutadiene (HTPB), is the primary cause of this change in mechanical characteristics. The HTPB binder molecules' oxidative crosslinking, a diffusion mechanism, is what governs this aging process [6]. Due to the widespread usage of solid propellant missiles throughout the armed services, these weapons must withstand a variety of handling, storage, and deployment circumstances. While missiles kept at a base significant temperature swings (up to more than 65°C), those stored in temperature variations throughout the day and throughout the year. A missile that has been launched from a jet aircraft has had to withstand temperatures that are substantially lower than those on the ground (as low as -50°C). The material experiences internal stresses and strains as a result of these temperature fluctuations [7]. The two most frequent failure modes are the propellant material breaking and the casing and propellant material deboning. High enough stresses and strains, repeated stresses and strains that weaken the material, (air) pockets created during the

construction process, as well as other causes that locally weaken the propellant can all cause cracking [8]. In this paper will organized, section 2. Methodology of design ultra sound detection based on laser vibration receiver; section 3 experimental steps, results and conclusion.

Materials that can store a lot of chemical energy are referred to be energetic materials. Once a chemical reaction releases this energy, the process may continue on its own without the aid of outside sources like oxygen. For instance, pyrotechnics, high explosives, and cannon and rocket propellants all employ these elements. The primary focus of this study effort will be on characterizing the aging of the latter [1].

Every branch of the military makes use of solid propellant missiles. Army, Navy, and Air Force missiles are launched by rocket engines .some armies possess missiles whose storage period has exceeded more than 26 years. Certain that these missiles are still secure for usage and storage [2]. Fuel and an oxidizer are the two fundamental components of solid propellants. This is combined with a binder, and then dried to form a solid propellant. Stabilizers, catalysts to speed up or slow down combustion, and plasticizers are further potential constituents [3].

2. Methods Methodology of Design Ultra Sound Detection Based on acoustic laser Receiver

The majority of non-contact ultrasound testing attempts use either air-coupled ultrasound or piezoelectric transducers placed in through-transmission. Optical excitation and ultrasonic detection in mode Laser Ultrasonic (LUS), is used appropriately [9]. The Laser pulses of nanosecond pulse width are absorbed, producing ultra-rapid ultrasound transients, either by ablation or a thermoplastic expansion followed by a relaxation [10]. Well-defined echoes are produced by these transients, and these echoes high temporal resolution to be used to separate them, allowing enabling using a suitably broad-bandwidth detector for single-sided testing technique. To do this today, most people rely on use the appropriate methods for measuring surface vibrations optical interferometers, providing detection bandwidths in 100 MHz [11]. This Laser Ultrasonic implementation has the drawback of having performance that is highly dependent on the optical qualities and surface features of the material being tested, both for excitation and for detection. Strongly scattering surfaces, for example, need powerful detection lasers and intricate interferometer setups, which may be expensive and challenging to miniaturize [12]. In this study, we describe a different approach based on the wide-range optical microphone and air-coupled detection of laser-induced ultrasound. Although detection this setup's bandwidth is constrained by ultrasonic attenuation in air [13], to frequencies between 10 Hz and 1 MHz, Still, it is ten times more powerful than modern air. Piezo transducers that are coupled are available. Therefore, one microsecond can be the length of an audio transient. They are precisely identified and spectrally and temporally separated. Analysis [14]. In figure 1 optical ultrasound laser microphone.

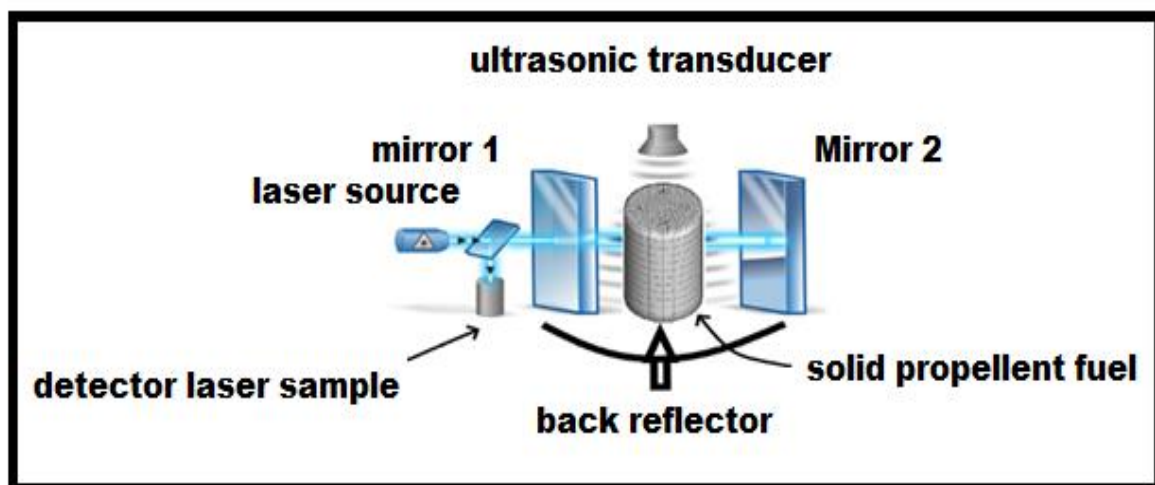


Figure 1. Optical laser microphone.

Visual microphone: detection theory. The refractive index of a media, which is a result of the local density, determines the wavelength of light in that medium. A stiff Fabry-Perot etalon may be used to detect this change in

optical wavelength since sound modulates density, which also affects density. The wavelength of the laser in the medium between the mirrors [15].

Which is measured by a photodiode, determines the intensity of the light reflected by the etalon. Surface qualities and optical properties of the sample are less important to the air-coupled detecting mechanism's operation. Although it is particularly well-suited to fiber-reinforced composite materials, and particularly sandwich structures, where ultrasound propagation at frequencies higher than 1 MHz is typically strongly attenuated, the measurements presented in the following show its applicability for non-destructive testing of steel parts [16].

3. Experimental Setup Environment

On ultrasonography and its uses in the realm of non-destructive testing, theoretical background is presented. The ability of ultrasonography to evaluate aging in solid propellant materials is anticipated. To examine some factors, feasibility and follow-up studies are conducted. The feasibility study's findings are used to create and fine-tune the follow-up studies [17]. Experiments. Pulse-echo measurements and tests will be used in the feasibility studies. The subsequent variables. Since it was anticipated that the inert propellant substance would significantly dampen the ultrasonic signal, samples with a thin thickness (5–30 mm) were made. All studies will be conducted using a pulse-echo setup [18]. This configuration was chosen because pulse-echo measurements would also be employed in the intended application of evaluating solid propellant rocket engines. Because of the cavity (bore hole) in the center of the engine, it is not possible to mount transducers within the motor to measure transmission, and it is also difficult to measure transmission along the whole diameter of the engine. The usage of the optimal frequency range and if the thicknesses chosen offer enough back reflections for additional investigation were tested through the feasibility trials. For the feasibility and follow-up investigations, inert propellant material samples were created [19]. As a result of safety rules banning non-certified products, inert materials are utilized. Individuals to carry or operate with reactive samples [20]. In the lack of a set recipe, an experimental approach is developed, and adjustments are made as necessary during the production process. The whole procedure is detailed in Appendix A, although this section just covers the key points. The samples were created in two batches. The initial batch consists of samples without a container that were applied to the feasibility tests. The samples from the second batch, which came in a container, were utilized in the studies that came next. The samples used in the subsequent tests were aged in a stove to simulate years of aging naturally [21]. The reactive (solid) particles that are bonded by hydroxyl-terminated polybutadiene (HTPB) are replaced with inert solid particles, in this case potassium sulfate, to match the composition of HTPB-based propellant material. Potassium sulfate, HTPB, and auxiliaries are combined with the binder at a ratio of 85:15. By using this ratio, the mixture is guaranteed to cure adequately and the solid particles won't migrate and gather at the bottom, leading to non-homogeneous samples [22]. The suggested non-contact laser-ultrasonic inspection technology was used. An ultrasonic detecting technique called pulse-echo was selected for the entire system. Echo is the signal that is picked up from the sample surface, whereas pulse is the creation of ultrasonic waves. Figure 2 depicts the Laser microphone system's experimental configuration. Table 1 lists the LUT settings applied to the target sample.

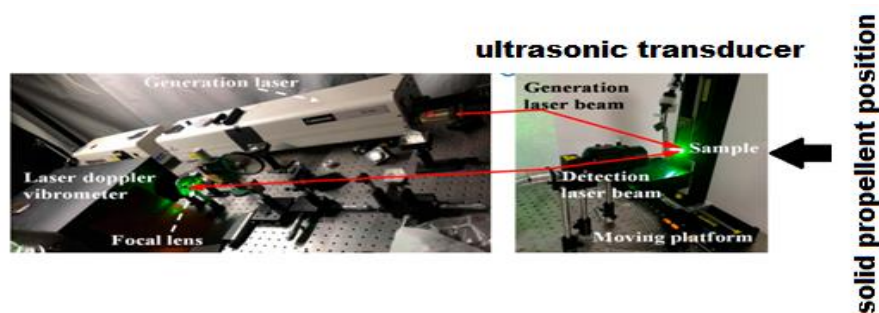


Figure 2. The proposed system of Laser microphone system's experimental configuration

The samples from the second batch, which were created following the feasibility studies, are included in Table 1. The containers used to cure the samples, as seen in Figure 3, The types of solid rocket fuel containers are divided

into two main types, the first is metal and the second is plastic polymers, according to the type of rocket, the method of propulsion and the interaction of the container with the combustion time, may be sealed airtight with a lid in storage case. In order to ensure that there is no air pollution surrounding the samples when not in use, the samples can now be sealed. All samples in a container have one surface exposed to the air, allowing the oxygen-induced aging process to only take place on one surface. Additionally, the container's bottom may now be used for ultrasonic measurements. Samples made for batch 2's trials are listed in Table 1.

Table 1. Ultrasonic measurements Samples

Sample	Thickness (mm)	Container	Aging temp
P1	17.05	Plastic	60°C
P2	17.90	Plastic	70°C
P3	16.65	Plastic	60°C
M1	9.30	Stainless steel	60°C
M2	15.70	Stainless steel	60°C
M3	20.40	Stainless steel	70°C

With the configuration used in these tests, the input signal can be tuned to either square wave or spike excitation. The most common waveform is a square wave with a length equal to half the frequency period of the transducer. That's exciting; the piezo element is energized at its resonant frequency by the tat signal. Excitement, a time less than this will result in an impossibly low and maximum capacity Citation period greater than this may cause oscillation distortion. Specifically, the length 500ns or 250ns, which is half the wavelength of 1MHz, or square input signal wave 500 kHz (1 second) or 1 second (0.5 second), respectively. The high excitation signal moves very quick.



Figure 3. Plastic and stainless steel containers for the solid propellant fuel respectively

4. Results

In these experiments, the grain anisotropy and grain-to-beam angle of a polycrystalline material can cause ultrasound that is propagating through it to be dispersed at grain boundaries. Typically, two occurrences may occur due of this encounter, a pen was created. First, the wave as it travels, due to the conversion of the will be somewhat muted several types of energy to sound energy. Second, a percentage of the reflected waveform will return to the sender. This backscattered or grain noises are terms used to describe observable energy. Conveys significant information about the microstructure and is noise-free, how it relates to the medium's physical characteristics for instance, grain size, texture, form, and orientation. Multiple attempts have reportedly improved understanding and modeling of back-signal refraction in polycrystalline materials Figure 4 3D image analysis of a perfect sample that does not have any defects (plastic and stainless steel casing), In this figure shows the semi-homogeneous cracks that are allowed in the sample after manufacturing, and that sample is considered the main reference for comparison with the following samples. In Figure 5 a cross section of solid rocket fuel shows heterogeneous cracks, with a three-dimensional image showing the amount of heterogeneous crack. The imaging was done through an ultrasound explorer based on a laser microphone to produce a very

accurate image of the cracks in the cross-section of the first sample, where the temperature, in which the test was performed to 60 degrees Celsius.

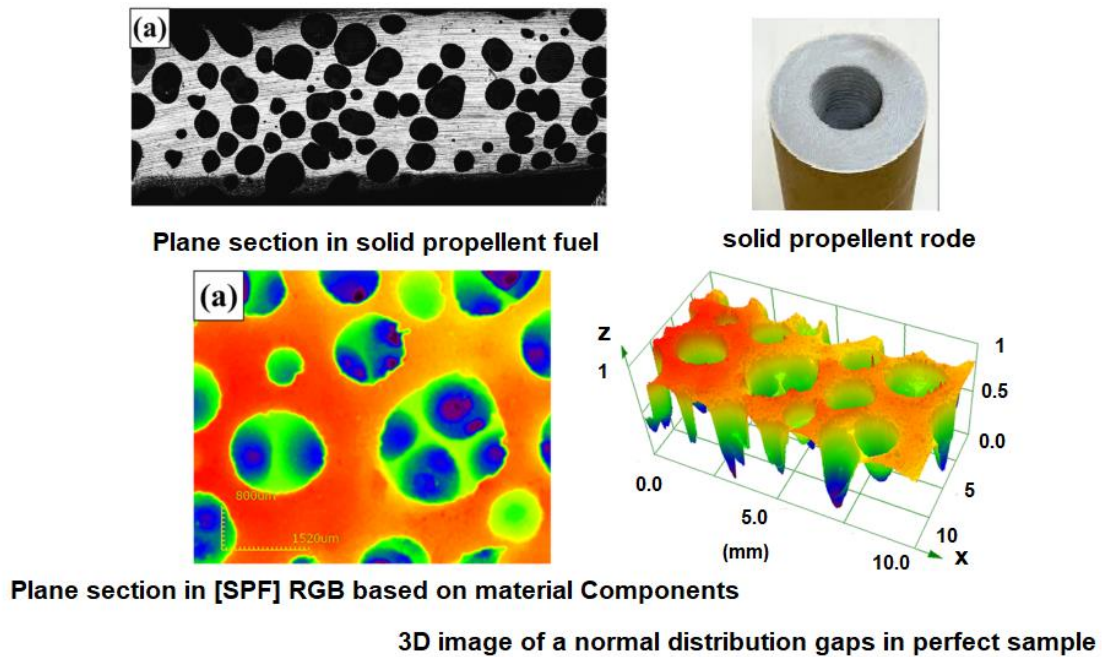


Figure 4. 3D image analysis of a perfect sample that does not have any defects (plastic and stainless steel casing).

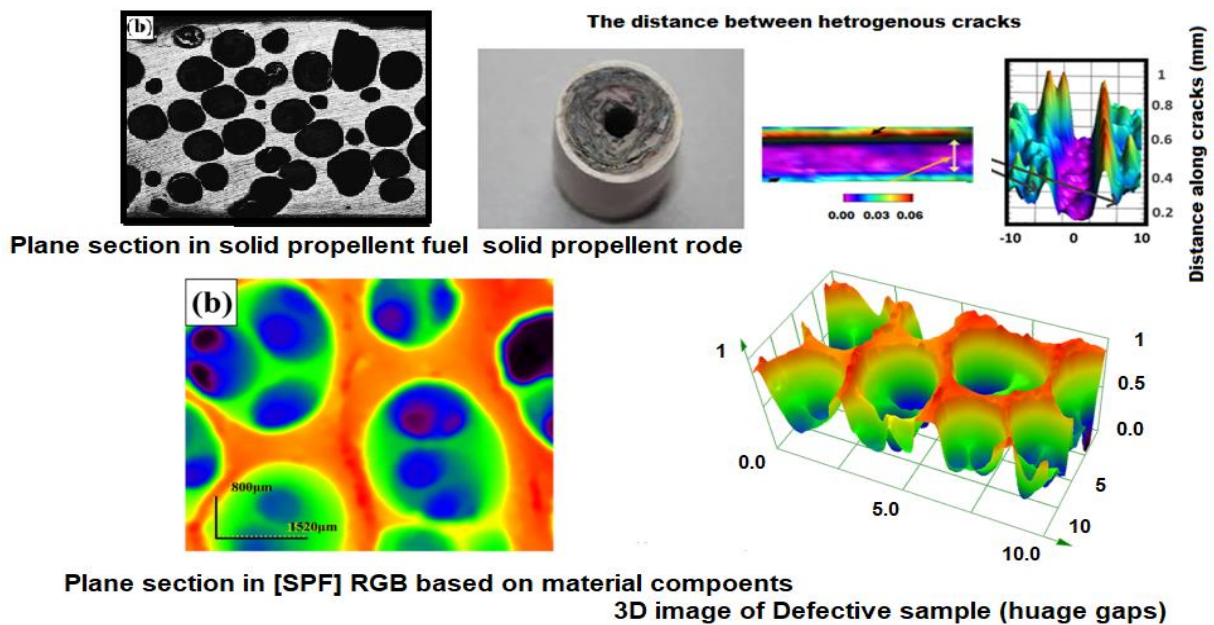


Figure 5. Heterogeneous cracks show in cross section of solid rocket fuel (plastic casing).

Commenting on the result reached using a laser receiver ultrasound diagnostic device, the first sample with a plastic shell has a thickness from 16.65: 17.6 mm. We will notice, that the cracks in the storage state in those casings of that thickness, work to make heterogeneous incisions by 5 mm transverse and 0.4 mm longitudinal at a temperature ranging from 60 to 70 degrees Celsius. Figure 6 shows solid fuel samples with stainless steel casings ranging in thickness between 9 and 20.4 mm, with a test temperature of 60 °C. In this diagnostic reading, heterogeneous cracks have reduced their transverse distances by 2 mm. While the number of heterogeneous slits longitudinally increased by 4 times than samples with plastic casing.

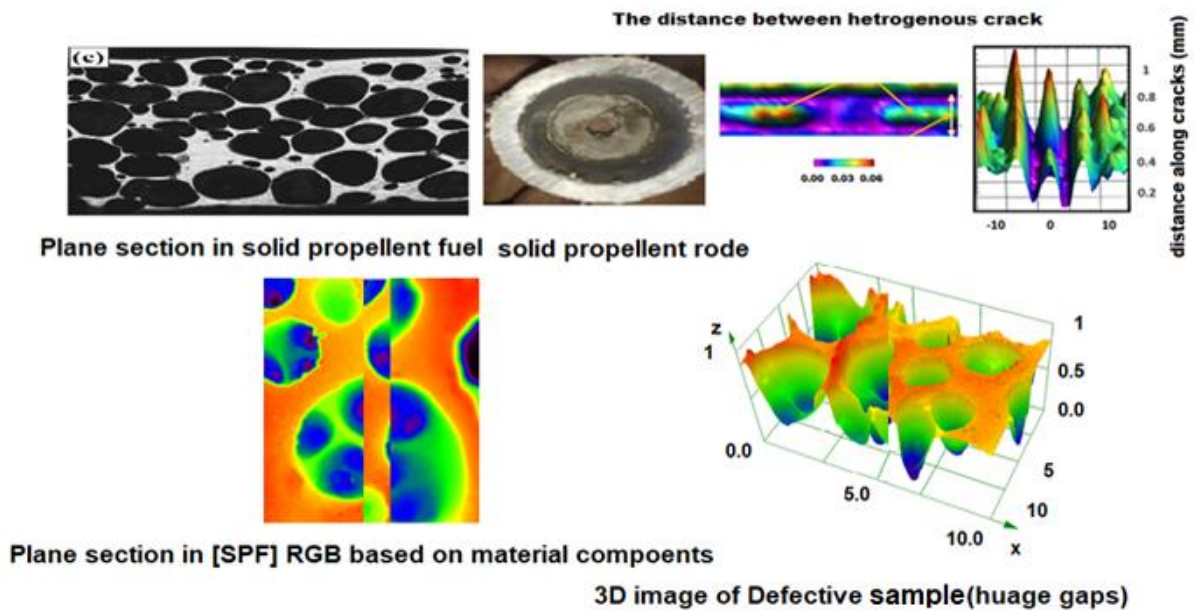


Figure 6. Heterogeneous cracks show in cross section of solid rocket fuel (stainless steel casing).

In Figure 7, 3D graph of a one heterogeneous crack in both cases shows the plastic casing and the stainless steel, Where the transverse heterogeneous cracks reached a diameter of 5 mm and 2 mm respectively, as it is clearly shown that the length of these heterogeneous cracks in the first case is 8 mm and the second case is 3 mm

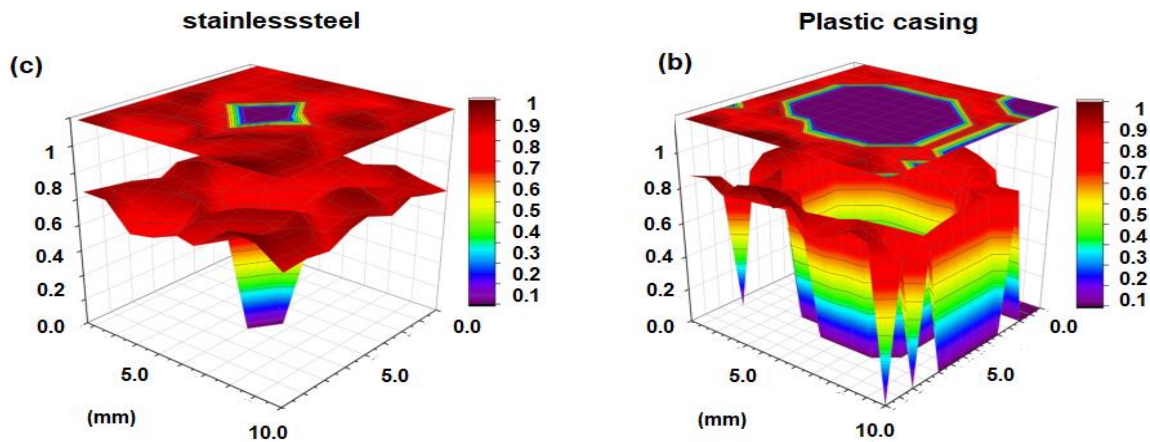


Figure 7. 3D graph of a one heterogeneous crack in both cases (plastic, stainless steel).

5. Conclusions

The system used to create a three-dimensional image to calibrate heterogeneous cracks in solid rocket fuel using laser ultrasonic receptors. The proposed system succeeded in telling us information about heterogeneous cracks that occur in solid rocket fuel in terms of transverse and longitudinal cracks. Where the longitudinal and transverse cracks with rocket fuel coated in plastic casings reached 0.4 mm and 5 mm, respectively. Heterogeneous cracks in rocket fuel coated with metal casings such as stainless steel amounted to 2 mm. At temperatures ranging from 50 to 70 degrees Celsius, this gives us an accurate understanding of what happens in rocket fuel when stored at such temperatures with various plastic and stainless steel casings. The future work in that area is to make temperature-resistant casings for solid rocket fuel systems based on those experiments that were done in this paper.

Declaration of Competing Interest: The authors declare that they have no known competing financial interests or personal relationships that could have appeared to influence the work reported in this paper.

Acknowledgments: The authors are very grateful to the members of the Communication and Electronics Engineering branch, Air Defense College, Cairo, Egypt for their encouragement, support, and help.

References

1. G. Gupta, L. Jawale; D. Mehilal; and B. Bhattacharya, Various methods for the determination of the burning rates of solid propellants: an overview. *Central European Journal of Energetic Materials* **2015**, vol. 12, pp. 593-620.
2. B. Duan; H. Zhang; Z. Hua; L. Wu; Z. Bao; N. Guo; et al., Burning characteristics and combustion wave model of AP/AN-based laser-controlled solid propellant. *Energy* **2022**, vol. 253, p. 124007.
3. J. V. Evans; B. T. Reid; R. M. Gejji; and C. D. Slabaugh, Solid-Fuel Ramjet Regression Rate Measurements Using X-Ray Radiography and Ultrasonic Transducers. *Journal of Propulsion and Power* **2023**, pp. 1-15.
4. Q. Wu; J. Liu; Y. Jin; Y. Chen; L. Du; and L. Waqas, Thickness measurement method for the thermal protection layer of a solid rocket motor based on a laser point cloud. *Insight-Non-Destructive Testing and Condition Monitoring* **2022**, vol. 64, pp. 219-228.
5. S. Mujeeb; and B. Karri, Experimental Validation of Composite Solid Propellant Burning Rate Prediction Model (He-Qu-1D) using Ultrasonic Burning Rate (UBR). *Indian Institute of Technology Hyderabad* **2019**.
6. F. Wang; J. Liu; B. Dong; J. Gong; W. Peng; Y. Wang; et al., Blind image separation for the deboning defects recognition of the solid propellant rocket motor cladding layer using pulse thermography. *Measurement* **2021**, vol. 174, p. 108997.
7. W. Xiong; Y. Liu; T. Zhang; S. Wu; D. Zeng; X. Guo; et al., Effect of Al-Li Alloy on the Combustion Performance of AP/RDX/Al/HTPB Propellant. *Aerospace* **2023**, vol. 10, p. 222.
8. V. Zarko; A. Kiskin; and A. Cheremisin, Contemporary methods to measure regression rate of energetic materials: A review. *Progress in Energy and Combustion Science* **2022**, vol. 91, p. 100980.
9. A. Y. Krainov; V. Poryazov; and K. Moiseeva, Numerical Simulation of the Nonstationary Burning of a Solid Propellant in the Combustion Chamber of a Controllable Solid-Propellant Propulsion System. *Journal of Engineering Physics and Thermophysics* **2022**, vol. 95, pp. 1604-1614.
10. P. Dermer; A. Varaksin; and A. Leontiev, The wall-free non-stationary fire whirls generation by axisymmetric burning of solid fuel pellets. *International Journal of Heat and Mass Transfer* **2017**, vol. 110, pp. 890-897.
11. A. Y. Krainov; V. Poryazov; and K. Moiseeva, Simulation of the Nonstationary Burning of a Solid Propellant in a Combustion Chamber and Calculation of the Acoustic Admittance of the Combustion Surface of this Propellant. *Journal of Engineering Physics and Thermophysics* **2023**, pp. 1-12.
12. V. Poryazov; A. Krainov; and D. Krainov, A mathematical model of metallized solid propellant combustion under the changing pressure. in *MATEC Web of Conferences* **2017**.
13. A. Y. Varaksin; A. Mochalov; and M. Romash, Experimental study of some characteristics of nonstationary wall-free fire whirls. *High Temperature* **2019**, vol. 57, pp. 738-743.
14. A. Ishchenko; E. Maslov; N. Skibina; and V. Faraponov, Complex investigation of nonstationary flow with shock waves in the working path of a hypersonic ramjet engine. *Journal of Engineering Physics and Thermophysics* **2021**, vol. 94, pp. 450-457.
15. A. Almslmany; E. A. Mohamed; O. A. omer; M. anwar; M. Alamir, A Promising Comprehensive Optical System Design and Fabrication for Solid-Fuel Characterization of the Missiles Engines. *Aswan University Journal of Sciences and Technology* **2023**, vol. 3, pp. 11-39.
16. E. A. Adel; O. A. Omer; M. Anwar; M. Alamir; M. Elhoshy; and A. Almslmany, A New Approach to Analyze Solid Fuel Exhaust for Rocket Engine Based on Laser Spectroscopy. in *2023 International Telecommunications Conference (ITC-Egypt)*, **2023**.
17. O. Glotov; V. Poryazov; G. Surodin; I. Sorokin; and D. Krainov, Combustion features of boron-based composite solid propellants. *Acta Astronautica* **2023**, vol. 204, pp. 11-24.
18. V. Kislov; M. Tsvetkov; A. Y. Zaichenko; D. Podlesniy; and E. Salgansky, Energy Efficiency of the Gasification of a Dense Layer of Solid Fuels in the Filter Combustion Mode, *Russian Journal of Physical Chemistry B* **2021**, vol. 15, pp. 819-826.
19. O. Orlandi; F. Fourmeaux; and J. Dupays, Ignition study at small-scale solid rocket motor. in *EUCASS* **2019**.
20. A. A. Gromov; K. V. Slusarsky; A. V. Sergienko; E. M. Popenko; E. L. Dzidziguri; K. B. Larionov; et al., Aluminized solid propellants loaded with metals and metal oxides: characterization, thermal behavior, and combustion. *Innovative Energetic Materials: Properties, Combustion Performance and Application* **2020**, pp. 157-182.
21. A. Lukin, New insights into the reactionary zones excited-state programming by plasma-acoustic coupling mechanism for the next-generation small satellite solid propulsion systems. in *Journal of Physics: Conference Series* **2020**.
22. J. V. Evans; B. T. Reid; R. M. Gejji; and C. D. Slabaugh, Solid-Fuel Ramjet Regression Rate Measurements Using X-Ray Radiography and Ultrasonic Transducers. *Journal of Propulsion and Power* **2022**, pp. 1-15.